Application of Kramers–Kronig relations to time–temperature superposition for viscoelastic materials

Lucie Rouleau, Jean-François Deü, Antoine Legay, Frédérique Le Lay

Application of Kramers–Kronig relations to time–temperature superposition for viscoelastic materials

L. Rouleau [a,b,*], J.-F. Deü [a], A. Legay [a], F. Le Lay [b]

[a] Structural Mechanics and Coupled Systems Laboratory, Conservatoire National des Arts et Métiers, 292 rue Saint-Martin, 75141 Paris, France
[b] Service Technique et Scientifique, DCNS Nantes-Indret, 44620 La Montagne, France

Dynamical mechanical analysis (DMA) is an experimental technique commonly used to study the frequency and temperature dependence of the mechanical properties of visco-elastic materials. The measured data are traditionally shifted by application of the time–temperature superposition principle to obtain the master curves of the viscoelastic mate-rial. The goal of this work is to present a methodology to determine the horizontal and ver-tical shift coefficients to be applied to the isotherms of storage and loss moduli measured. The originality lies in the calculation of the shift coefficients by a method requiring fulfil-ment of the Kramers–Kronig relations conveying the causality condition. The computed vertical shift coefficients are compared to the coefficients predicted by the Bueche–Rouse theory.

1. Introduction

Viscoelastic materials are extensively used in industrial applications for noise and vibration reduction. A good representation of their mechanical properties is required in order to predict and optimise structures integrating such materials. Viscoelastic materials present a temperature and frequency dependence of their mechanical properties. Dynamical mechanical analysis (DMA) is a common technique to characterise materials as a function of temperature and frequency, but due to the limitations of the measurement instruments, only a reduced frequency range can be investigated. To know the material behaviour on a broader frequency range, the time–temperature superposition (TTS) principle is classically applied (Ferry, 1980; Emri, 2005; Dealy and Plazek, 2009). It stipulates that for some materials, termed as thermo-rheologically simple (TRS), data at different temperatures T can be shifted vertically and horizontally to obtain the master curves of the material on a wide frequency range at a chosen reference temperature T_0. The temperature-dependent shift coefficients $a_T(T, T_0)$ govern the horizontal shifts by multiplying the frequency for each isotherm, while the temperature-dependent shift coefficients $b_T(T, T_0)$, applied to the storage and loss moduli, dictate the vertical shifts (see Eq. (11) in Section 2.3).

The horizontal shift coefficients can be estimated by the WLF (Williams–Landel–Ferry) equation which gives an empirical expression of the temperature-dependent function $a_T(T, T_0)$ (Williams et al., 1955). But they are usually determined by "hand-shifting" (Ferry, 1980) or by curve fitting techniques (Sihn and Tsai, 1999; Gergesova et al., 2011; 01dB-Metravib) in order to best superimpose the isotherms. The former is subjective and lacks of precision while the latter is more reliable since the procedure is automated. However, both techniques do not give any physical meaning to the shift coefficients and are prone to errors due to fitting procedures. Some authors have proposed other methods in which the shift coefficients are identified along the parameters of a viscoelastic model (Fowler and Rogers, 2004; Madigosky et al., 2006; Guedes, 2011). This way, the calculated

* Corresponding author at: Structural Mechanics and Coupled Systems Laboratory, Conservatoire National des Arts et Métiers, 292 rue Saint-Martin, 75141 Paris, France. Tel.: +33 1 40272328; fax: +33 1 40272716.
E-mail address: lucie.rouleau@cnam.fr (L. Rouleau).

shift coefficients have a physical meaning since the viscoelastic model is supposed to verify some conditions such as causality (Pritz, 1999). However, it requires to set a priori the material modulus function. If the chosen viscoelastic model is not the most appropriate to model the frequency dependence of the mechanical properties of the viscoelastic material, it may lead to significant discrepancies between the experiments and the model. In Caracciolo et al. (2001) and Chailleux et al. (2006), the horizontal shift coefficients are determined thanks to the approximated Kramers–Kronig relations described in Booij and Thoone (1982), linking the storage and the loss moduli. In both cases, this method gives satisfactory results but has limited use due to the assumed approximations.

The vertical shift coefficients represent the temperature-dependence of the modulus. This dependence is usually weak and the coefficients are often taken as unity. However, some materials exhibit a need for vertical shifting. These shifting coefficients can be determined for best visual superposition of the isotherms (Ferry, 1980; Fowler and Rogers, 2006) or by identification of a viscoelastic model (Guedes, 2011). The drawbacks of these methods have already been cited. Another kind of method is an application of the Bueche–Rouse theory of linear viscoelasticity to estimate the vertical shift factors from measurements of the temperature variation of the modulus or of the density. For example, in Resh et al. (2009), the steady state compliance of a polymer is measured at various temperatures. The efficiency of this class of method relies on the precision of the measurements.

The purpose of this work is to present an original method to generate master curves consistent with the principle of causality, without requiring an a priori material's modulus function. In a first step, horizontal coefficients are determined with a classical least square method, and vertical shift coefficients set to unity. After this initialisation, the shift coefficients are optimised such that the Kramers–Kronig relations are best verified. This method ensures that the built master curves fulfil the best the Kramers–Kronig causality conditions. It is applied to DMA measurements of Deltane 350, a polymer from Paulstra®. The vertical shift coefficients calculated with the proposed method are compared to those predicted from the Bueche–Rouse theory, calculated from measurements of the density with temperature.

2. Theory of viscoelasticity

This first section recalls the definition and the calculation of the Kramers–Kronig relations, as well as the time–temperature superposition principle, which are the key points of the shifting method presented in the next section. The Williams–Landel–Ferry equation and the Bueche–Rouse theory which can be used to make a critical study of the optimised shift coefficients are also exposed.

2.1. Kramers–Kronig causality relations

The frequency and temperature dependence of the viscoelastic material's properties can be described by a complex modulus $G^*(\omega)$:

$$G^*(\omega) = G'(\omega) + \mathrm{i}G''(\omega) = |G^*(\omega)| \exp(\mathrm{i}\phi(\omega)) \tag{1}$$

where $G'(\omega)$ and $G''(\omega)$ are the storage and loss moduli, $|G^*(\omega)|$ is the amplitude and $\phi(\omega)$ is the phase angle. In the context of linear viscoelasticity, the constitutive law which links the stress σ to the strain ϵ can be written in its convolution integral form (Christensen, 2003):

$$\sigma(t) = \int_{-\infty}^{t} G(t-\tau) \frac{\mathrm{d}\epsilon(\tau)}{\mathrm{d}\tau} \mathrm{d}\tau \tag{2}$$

If the initial strain is $\epsilon(t) = 0$ for $t < 0$, and the modulus is written as:

$$G(t) = G(t \to 0) - h(t), \tag{3}$$

the stress–strain relationship becomes:

$$\sigma(t) = G(t \to 0)\epsilon(t) - \int_{-\infty}^{t} h(t-\tau) \frac{\mathrm{d}\epsilon(\tau)}{\mathrm{d}\tau} \mathrm{d}\tau \tag{4}$$

The causality condition requires the memory function $h(t)$ to be causal, i.e. $h(t) = 0,\ \forall t < 0$. The Fourier transform of a real linear causal function $h(t)$ that does not possess any singularity at $t = 0$ respects certain relations between its real and imaginary parts (Champeney, 1973):

$$\begin{aligned} \Re(h^*(\omega)) &= \frac{2}{\pi} \int_0^{\infty} \frac{u\Im(h^*(u))}{\omega^2 - u^2} \mathrm{d}u \\ \Im(h^*(\omega)) &= \frac{2\omega}{\pi} \int_0^{\infty} \frac{\Re(h^*(u))}{u^2 - \omega^2} \mathrm{d}u \end{aligned} \tag{5}$$

Using Eq. (1) and the Fourier transform of Eq. (3) ($G^*(\omega) = G_\infty - h^*(\omega)$) in Eq. (5) leads to the so-called Kramers–Kronig relations linking the real and the imaginary parts of the complex modulus (Kramers, 1927; Kronig, 1926; Silva and Gross, 1941):

$$G'(\omega) = G_\infty + \frac{2}{\pi} \int_0^{\infty} \frac{uG''(u)}{\omega^2 - u^2} \mathrm{d}u \tag{6a}$$

$$G''(\omega) = \frac{2\omega}{\pi} \int_0^{\infty} \frac{G'(u)}{u^2 - \omega^2} \mathrm{d}u \tag{6b}$$

where $G_\infty = G^*(\omega \to \infty) = G(t \to 0)$ is the unrelaxed modulus. Similar equations link the logarithm of the modulus' amplitude to the phase angle:

$$\ln(|G^*(\omega)|) = \ln(|G_\infty|) + \frac{2}{\pi} \int_0^{\infty} \frac{u\phi(u)}{\omega^2 - u^2} \mathrm{d}u \tag{7a}$$

$$\phi(\omega) = \frac{2\omega}{\pi} \int_0^{\infty} \frac{\ln(|G^*(u)|)}{u^2 - \omega^2} \mathrm{d}u \tag{7b}$$

The Kramers–Kronig equations are a necessary and sufficient condition for causality (Enelund and Olsson, 1999).

2.2. Numerical calculation of the Kramers–Kronig relations

Booij and Thoone (1982) propose a first approximation of the Kramers–Kronig relations by making assumptions on the monotony of the functions to be integrated:

$$G''(\omega) \approx \frac{\pi}{2} \left(\frac{\mathrm{d}G'(u)}{\mathrm{d}\ln u} \right)_{u=\omega} \tag{8a}$$

$$G'(\omega) - G'(0) \approx -\frac{\omega\pi}{2}\left(\frac{\mathrm{d}[G''(u)/u]}{\mathrm{d}\ln u}\right)_{u=\omega} \tag{8b}$$

$$\phi(\omega) \approx \frac{\pi}{2}\left(\frac{\mathrm{d}\ln|G^*(u)|}{\mathrm{d}\ln u}\right)_{u=\omega} \tag{8c}$$

These approximated relations are used in Caracciolo et al. (2001) to calculate the phase angle from measurements of the amplitude of the modulus. But they do not involve any integration, and in Parot and Duperray (2007) it is shown that this approach is not good enough to deal with experimental measurements since it introduces important noise in the computed responses. Instead, Parot and Duperray (2007) propose a numerical method to evaluate the exact Kramers–Kronig relations of Eqs. (6) and (7). The outline of this method is exposed here and the reader is referred to Parot and Duperray (2007) for more details. Let us consider n measurements of $\ln(|G^*|)$ and ϕ at the frequencies $(\omega_i)_{1..n}$. The first step is to average the logarithm of the modulus' amplitude and the phase angle over the next two neighbours to obtain smooth functions $\ln(|G^*|)$ and ϕ evaluated at the middle point measurement frequencies. The second step is to extend these functions to continuous functions on the domain of integration $[0, +\infty[$:

- $\ln(|G^*|)$ is an even function that is assumed to be constant at high and low frequencies to account for the slow modulus' variations observed in the rubbery plateau and the glassy zone:
$$\ln(|G^*(\omega)|) = \ln(|G^*(\omega_1)|), \quad \forall\omega \in [0, \omega_1]$$
$$\ln(|G^*(\omega)|) = \ln(|G^*(\omega_n)|), \quad \forall\omega \in [\omega_n, +\infty[$$
- ϕ is an odd function that is equal to zero at $\omega = 0$ since the complex modulus is real at $\omega = 0$ (static modulus). It is assumed to vary linearly on $[0, \omega_1]$ and to be constant on $[\omega_n, +\infty[$. Although devoid of physical meaning, these reasonable simple assumptions allow an easy analytical integration of the Kramers–Kronig relations:
$$\phi(\omega) = \phi(\omega_1)\frac{\omega}{\omega_1}, \quad \forall\omega \in [0, \omega_1]$$
$$\phi(\omega) = \phi(\omega_n), \quad \forall\omega \in [\omega_n, +\infty[$$

The justification of these extensions are based on the parity of the functions $\ln(|G^*|)$ and ϕ. The discretized interval of integration is composed of the middle point measurement frequencies, the limit of integration 0 and $+\infty$, and two added points $\omega_1/2$ and $\omega_n + (\omega_n - \omega_{n-1})/2$:

$$[\Omega_0 = 0,\ \Omega_1 = \frac{\omega_1}{2},\ \Omega_2 = \frac{\omega_2 + \omega_1}{2}, \ldots,\ \Omega_n = \frac{\omega_{n-1} + \omega_n}{2}, \Omega_{n+1} = \omega_n + \frac{\omega_n - \omega_{n-1}}{2}, \Omega_{n+2} = +\infty[$$

The functions $\ln(|G^*|)$ and ϕ are assumed to be linear on each interval:

$$\begin{cases} \ln(|G^*(\omega)|) = a_i\omega + b_i, & \text{on } [\Omega_i, \Omega_{i+1}] \\ \phi(\omega) = c_i\omega + d_i, & \text{on } [\Omega_i, \Omega_{i+1}] \end{cases} \tag{9}$$

The diagrams in Fig. 1 explain the process of smoothing, extension and linearisation of the functions $\ln(|G^*|)$ and ϕ to be integrated. After numerical integration of Eqs. (7a) and (7b), using the relations (9), one gets:

$$\begin{aligned} \ln(|G^*(\omega)|) - \ln(|G_\infty|) = &-\frac{2c_0}{\pi}\Omega_1 - \frac{c_0\omega}{\pi}\ln\left|\frac{\Omega_1 - \omega}{\Omega_1 + \omega}\right| \\ &- \sum_{i=1}^{n}\left[\frac{2c_i}{\pi}(\Omega_{i+1} - \Omega_i) + \frac{c_i\omega}{\pi}\ln\left|\frac{(\Omega_{i+1} - \omega)(\Omega_i + \omega)}{(\Omega_{i+1} + \omega)(\Omega_i - \omega)}\right|\right. \\ &\left. + \frac{d_i}{\pi}\ln\left|\frac{\Omega_{i+1}^2 - \omega^2}{\Omega_i^2 - \omega^2}\right|\right] \\ \phi(\omega) = &\frac{b_0}{\pi}\ln\left|\frac{\Omega_1 - \omega}{\Omega_1 + \omega}\right| + \sum_{i=1}^{n}\left[\frac{a_i\omega}{\pi}\ln\left|\frac{\Omega_{i+1}^2 - \omega^2}{\Omega_i^2 - \omega^2}\right|\right. \\ &\left. + \frac{b_i}{\pi}\ln\left|\frac{(\Omega_{i+1} - \omega)(\Omega_i + \omega)}{(\Omega_{i+1} + \omega)(\Omega_i - \omega)}\right|\right] + \frac{b_{n+1}}{\pi}\ln\left|\frac{\Omega_{n+1} + \omega}{\Omega_{n+1} - \omega}\right| \end{aligned} \tag{10}$$

This method allows the calculation of the phase angle from the amplitude of the modulus and vice versa. The accuracy of the integrals' calculation depends on the frequency range on which is performed the integration, the density and the repartition of measurement points. The former must be large enough to justify the extensions made on the functions $\ln(|G^*|)$ and ϕ. The latters have an influence on the validity of the linear assumption made on each interval of integration discretised. This method will be used in Section 3.2 to compute the amplitude and the phase angle from the Kramers–Kronig relations and the horizontally shifted experimental data.

2.3. Time–temperature superposition principle

The classically applied time–temperature superposition principle involves only the horizontal shift coefficients a_T, and gives an equivalence between the mechanical properties measured at a frequency f and a temperature T and the mechanical properties at a reduced frequency f_r and a reference temperature T_0. However for some materials, the introduction of vertical shift coefficients (denoted b_T) is necessary. In its general form, the time–temperature superposition principle can be summarised as this:

$$\begin{aligned} f_r &= a_T(T, T_0)f \\ G'(f_r, T_0) &= b_T(T, T_0)G'(f, T) \\ G''(f_r, T_0) &= b_T(T, T_0)G''(f, T) \end{aligned} \tag{11}$$

where f_r is the reduced frequency and T_0 is the reference temperature. Fig. 2 represents the time–temperature principle. The time–temperature superposition principle applies when the material is said to be thermo-rheologically simple, which means that the same shift factors are applied to all relaxation times, and when the temperature dependence of the shift coefficients has a reasonable form (Arrhenius, WLF) (Ferry, 1980). A good indication of thermo-rheological simplicity is to look at the Cole–Cole plot (Han and Kim, 1993) (loss modulus $G''(\omega)$ versus storage modulus $G'(\omega)$) or the wicket plot (Van Gurp and Palmen, 1998) (loss angle $\phi(\omega)$ versus modulus' magnitude $|G^*(\omega)|$). As long as all data lie close to one

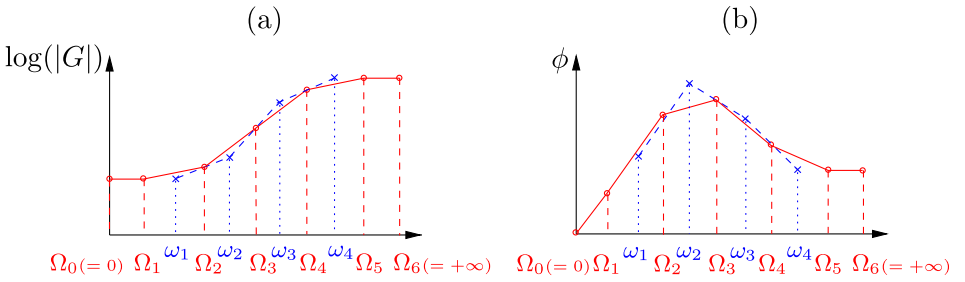

Fig. 1. Smoothing, extension and linearisation of the functions $\ln(|G^*|)$ (a) and ϕ (b).

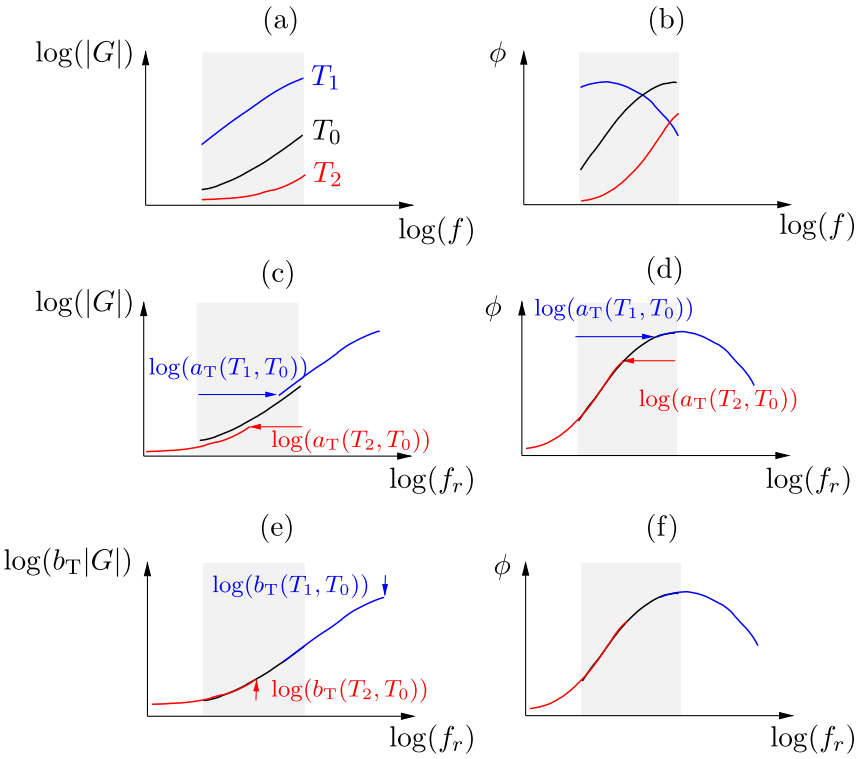

Fig. 2. Time–temperature superposition principle. (a), (b) Isotherms of the complex modulus amplitude and the phase angle on a limited frequency range with $T_1 < T_0 < T_2$. (c), (d) Horizontal shifting of the isotherms of complex modulus amplitude and the phase angle with T_0 the reference temperature. (e), (f) Vertical shifting of the isotherms of complex modulus amplitude with T_0 the reference temperature.

curve, the requirements for thermo-rheological simplicity are fulfilled. These plots also identify the need for vertical shifting: if the plots exhibit a slight temperature dependence like parallel isotherms, then vertical shifting is necessary.

The Williams–Landel–Ferry equation (WLF) is an empirical equation (Williams et al., 1955) for the temperature-dependent horizontal shift coefficients, based on the assumption that the fractional free volume of polymers increases with temperature:

$$\log(a_T(T, T_0)) = \frac{-C_1(T - T_0)}{C_2 + T - T_0} \tag{12}$$

where C_1 and C_2 are empirical coefficients that are found of the order of magnitude 10 and 100 respectively (Ferry, 1980; Williams et al., 1955). These values of C_1 and C_2 vary from one material to another, but the horizontal shift coefficient usually comply reasonably well with the WLF equation (Madigosky et al., 2006; Fowler and Rogers, 2004; Guedes, 2011; Bossemeyer, 2001), and a good fit is commonly associated to coherent values of the horizontal shift coefficients.

The Bueche–Rouse theory is explaining the polymer chain motion of unentangled polymers in the context of linear viscoelasticity (Dealy and Wissbrun, 1990; Bueche, 1954). This theory predicts that the relaxation modulus is proportional to ρT, where ρ and T are the density of the polymer and the temperature respectively. Since the vertical shift coefficients reflect the temperature dependence of the modulus of the viscoelastic material, they can be expressed as (Dealy and Plazek, 2009):

$$b_T(T,T_0)=\frac{T_0\rho_0}{T\rho} \tag{13}$$

where ρ_0 refers to the density of the material at the reference temperature T_0. Assuming that the mass of the material remains constant during the DMA measurements leads to the following expression of the vertical shift coefficients:

$$b_T(T,T_0)=\frac{T_0}{T}(1+\alpha(T-T_0))^3 \tag{14}$$

where α is the linear thermal expansion coefficient of the material. Knowing this coefficient, the Bueche–Rouse theory can be applied to give an estimation of the vertical shift coefficients.

3. Determination of the shift coefficients

In this section the optimisation procedure used to determine both the horizontal and vertical shift coefficients is presented. The first step is to chose an appropriate starting point for the algorithm. It is presented in Section 3.1. The second step is to optimise the coefficients by minimising a criterion based on the Kramers–Kronig relations. This is developed in Section 3.2. The optimised coefficients can be compared to those predicted by the known theories presented in the previous section.

3.1. Starting point

The analytical integration of the Kramers–Kronig relations requires the modulus' amplitude and the phase angle to be continuous functions over a broad reduced frequency range representative of the interval of integration $[0,+\infty]$ (the functions are then extended to $[0,+\infty]$). For that reason, it is important that the starting shift coefficients produce almost superimposed isotherms. The starting horizontal shift coefficients $\mathbf{a}_T^0$ are taken as the set of parameters minimising the norm of a cost function $\mathbf{F}_0$ representing the deviation of the shifted experimental points from a polynomial fitted curve:

$$\mathbf{a}_T^0=\left\{\mathbf{x}\middle|\min_{\mathbf{x}}\left(\sum_{i=1}^{n_f}|F_0(\mathbf{x},f_r^i)|^2\right)\right\} \tag{15}$$

Experimental measurements of the modulus are performed on the frequency range $\mathbf{f}=[f_1,f_2,\ldots,f_{n_f}]$ and the temperature range $\mathbf{T}=[T_1,T_2,\ldots,T_{n_T}]$. This leads to a cloud of $n=n_T\times n_f$ measurement points. For a given set of parameters $\mathbf{x}=[a_T(T_1),\ldots,a_T(T_{n_T})]$, the time–temperature superposition principle is applied to experimental data to obtain shifted data:

$$\begin{aligned} &f_r^i=a_T(T_j)f_k\\ &\ln(|G^*_{shift}(\mathbf{x},f_r^i(\mathbf{x}))|)=\ln(b_T(T_j))+\ln(|G^*_{exp}(T_j,f_k)|)\\ &\phi_{shift}(\mathbf{x},f_r^i(\mathbf{x}))=\phi_{exp}(T_j,f_k) \end{aligned} \tag{16}$$

where $i=1\ldots n$, $j=1\ldots n_T$ and $k=1\ldots n_f$. The shifted data are then fitted by a polynomial. Since the storage and loss moduli G'_{shift} and G''_{shift} are found to be more easily fitted by a polynomial than $\ln(|G^*_{shift}|)$ and ϕ_{shift}, the cost function is defined as:

$$\begin{aligned} F_0(\mathbf{x},f_r^i)&=\frac{G*_{shift}(\mathbf{x},f_r^i(\mathbf{x}))-G^*_{fit}(\mathbf{x},f_r^i(\mathbf{x}))}{G^*_{shift}(\mathbf{x},f_r^i(\mathbf{x}))}\\ &=\frac{G\prime_{shift}(\mathbf{x},f_r^i(\mathbf{x}))+iG''_{shift}(\mathbf{x},f_r^i(\mathbf{x}))-G'_{fit}(\mathbf{x},f_r^i(\mathbf{x}))-iG''_{fit}(\mathbf{x},f_r^i(\mathbf{x}))}{G'_{shift}(\mathbf{x},f_r^i(\mathbf{x}))+iG''_{shift}(\mathbf{x},f_r^i(\mathbf{x}))} \end{aligned} \tag{17}$$

where G'_{shift} and G''_{shift} are the polynomial fit of G'_{shift} and G''_{shift} respectively. The horizontal shift coefficient at the reference temperature $\mathbf{a}_T(T_0)$ is set to unity. For many materials the vertical shift coefficients are close to unity, and are generally smaller than the horizontal shift coefficients by at least one order of magnitude (Guedes, 2011; Fowler and Rogers, 2006). So the starting coefficients are set to unity. Another possibility would be to initialize the vertical shift coefficients from Eq. (14), after measuring the thermal expansion coefficient.

3.2. Optimisation process

According to the causality principle, the modulus' amplitude and the phase angle of a linear viscoelastic material are linked by the Kramers–Kronig relations. The goal of the optimisation process is to find the shift coefficients producing the best master curves according to those relations. The optimised shift coefficients are the ones minimising a cost function $\mathbf{F}$ representing the discrepancies between the experimental shifted modulus and the modulus computed by the Kramers–Kronig relations:

$$[\mathbf{a}_T^{opt},\mathbf{b}_T^{opt}]=\left\{\mathbf{x}\middle|\min_{\mathbf{x}}\sum_{i=1}^{n_f}|F(\mathbf{x},f_r^i)|^2\right)\right\} \tag{18}$$

For a given set of parameters $\mathbf{x}=[a_T(T_1),\ldots,a_T(T_{n_T}),b_T(T_1),\ldots,b_T(T_{n_T})]$, the time–temperature superposition principle is applied to experimental data to obtain shifted data as in Eq. (16). The functions $\ln(|G^*_{shift}|)$ and ϕ_{shift} are first smoothed and extended on the interval $[0,+\infty[$ ($G^*_{int}|$ and ϕ_{int}), then numerically integrated in the Kramers–Kronig relationships, as described in Section 2.2:

$$\begin{aligned} \ln(|G^*_{KK}(\mathbf{x},f_r)|)&=\ln(|G^*_{int_\infty}|)+\frac{2}{\pi}\int_0^\infty\frac{u\phi_{int}(\mathbf{x},u)}{f_r^2-u^2}du\\ \phi_{KK}(\mathbf{x},f_r)&=\frac{f_r}{\pi^2}\int_0^\infty\frac{\ln(|G^*_{int}(\mathbf{x},u)|)}{u^2-f_r^2}du \end{aligned} \tag{19}$$

Exact verification of the Kramers–Kronig relationship corresponds to $\ln(G^*_{KK})=\ln(G^*_{shift})$. The cost function to be minimised is defined as:

$$\begin{aligned} F(\mathbf{x},f_r^i)&=\frac{\ln(G^*_{shift}(\mathbf{x},f_r^i(\mathbf{x})))-\ln(G^*_{KK}(\mathbf{x},f_r^i(\mathbf{x})))}{\ln(G^*_{shift}(\mathbf{x},f_r^i(\mathbf{x})))}\\ &=\frac{\ln(|G^*_{shift}(\mathbf{x},f_r^i(\mathbf{x}))|)+i\phi_{shift}(\mathbf{x},f_r^i(\mathbf{x}))-\ln(|G^*_{KK}(\mathbf{x},f_r^i(\mathbf{x}))|)}{\ln(|G^*_{shift}(\mathbf{x},f_r^i(\mathbf{x}))|)+i\phi_{shift}(\mathbf{x},f_r^i(\mathbf{x}))}\\ &\quad-\frac{i\phi_{KK}(\mathbf{x},f_r^i(\mathbf{x}))}{\ln(|G^*_{shift}(\mathbf{x},f_r^i(\mathbf{x}))|)+i\phi_{shift}(\mathbf{x},f_r^i(\mathbf{x}))} \end{aligned} \tag{20}$$

Any viscoelastic model can then be identified on the obtained master curves. This approach allows a simultaneous and automatic determination of both horizontal and vertical shift coefficients directly from DMA measurements.

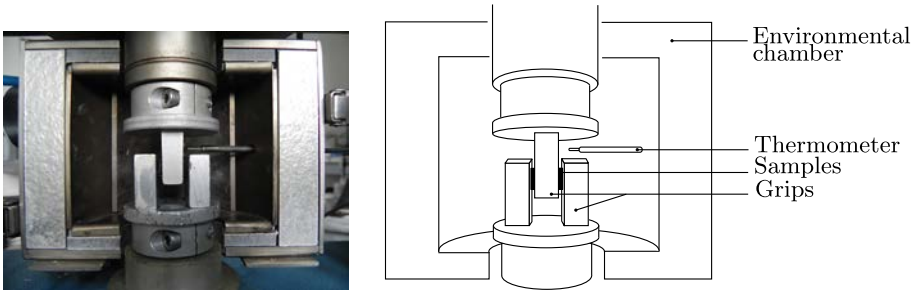

Fig. 3. DMA Metravib 450+ in a shear mode configuration. A sinusoidal displacement is applied to the sample and the shear stress is measured. The environmental chamber allows to make measurements at different temperatures.

4. Results and discussion

4.1. DMA measurements

The viscoelastic material used in this study is Deltane 350, an amorphous polymer supplied by Paulstra®. DMA measurements are carried out on a Metravib DMA 450+ with the testing configuration in the shear mode, as shown on Fig. 3. Specimen of size 9 mm × 6 mm × 2 mm are first excited at 10 Hz, over the temperature range −80 °C to 70 °C with a heating rate of 2 °C/min. This allows the determination of the glass transition temperature $T_g = -10$ °C. The specimen are then tested in the frequency range 0–400 Hz ($n_f = 10$ measurement points), and over the temperature range −40 °C to 43 °C ($n_T = 18$ measurement points) with a heating rate of 2 °C/min. A dynamic displacement of 5 μm is applied to the specimen to remain in the linear viscoelastic domain.

The validity of the time–temperature superposition principle for Deltane 350 is checked by way of the wicket plot, shown on Fig. 4, and the Cole–Cole plot, shown on Fig. 5, obtained from the DMA measurements. Both figures show a slight temperature dependence of the material's properties, which indicates a need for vertical shifting. It is reminded that the wicket and the Cole–Cole plots remain unaffected by a change in the horizontal shift coefficients.

4.2. Obtention of the master curves

The method presented above is applied to the DMA measurements for Deltane 350 to determine the horizontal and vertical shift coefficients. The reference temperature chosen for the application of the time–temperature superposition principle is the operating temperature $T_0 = 12$ °C. The master curves obtained are given on Fig. 6. A reasonably good superposition is achieved although the points corresponding to the three coldest isotherms do not superimpose well with the others. The same observation can be made by looking at Fig. 4. As the vertical shift coefficients do not apply to the phase angle, the problem is transferred on the master curves.

Fig. 7 compares the experimental modulus' amplitude and phase angle to their counterparts calculated by analytical integration of the Kramers–Kronig relations, at the first step of the optimisation. The chosen starting shift coefficients give quite good results since the experimental val-

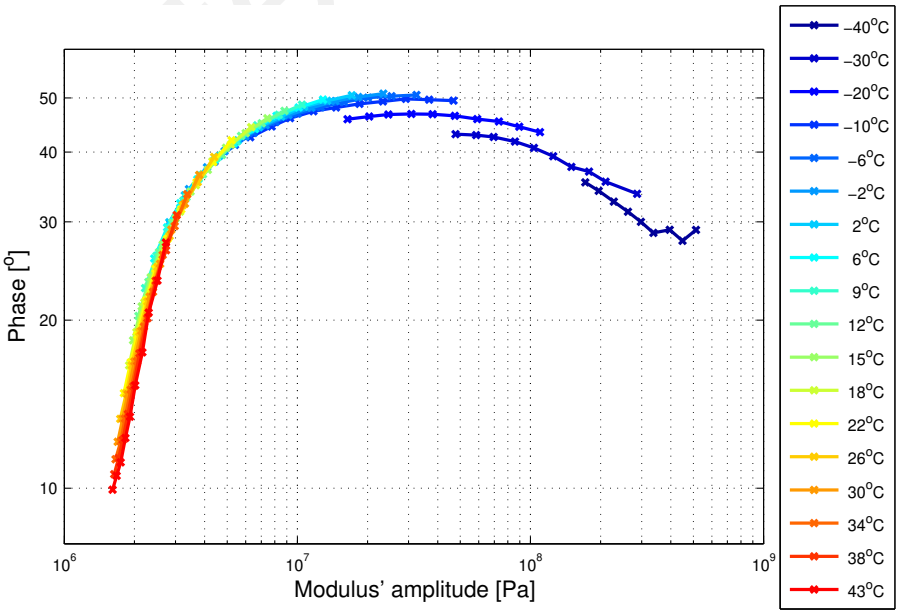

Fig. 4. Wicket plot for Deltane 350.

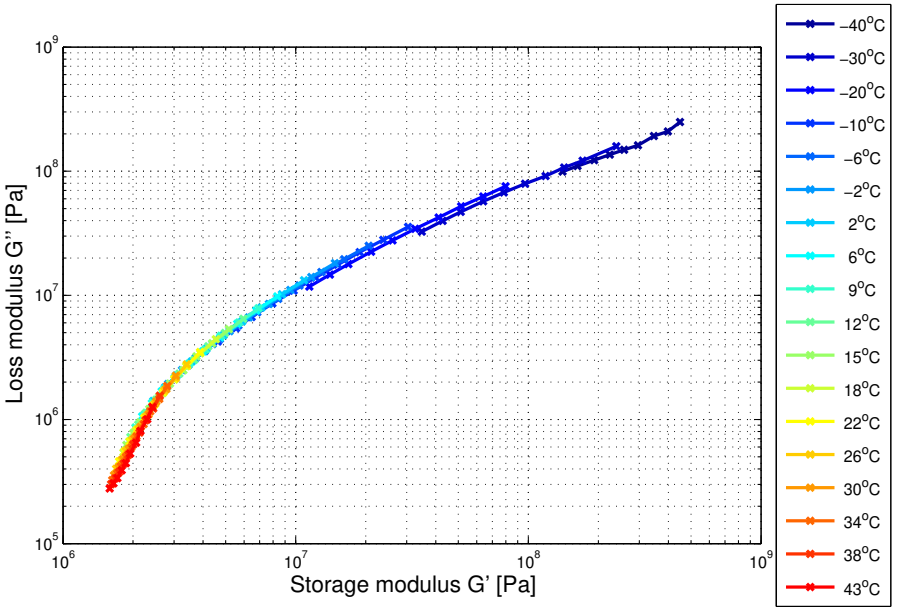

Fig. 5. Cole–Cole plot for Deltane 350.

ues are close to the computed values. However, Fig. 7 shows differences in the static modulus ($G^*(\omega \to 0)$) and in the frequency and peak value of the phase angle.

The same comparison is made at the end of the optimisation (see Fig. 8) and the results are greatly improved. The good superposition between the two curves shows that the master curves obtained at the end of the optimisation are consistent with the Kramers–Kronig relations. The small errors on the phase angle at low and high frequency are due to border effects when integrating analytically the Kramers–Kronig relations. This can be improved by investigating temperatures at colder and higher temperatures.

4.3. Analysis of the optimised shift coefficients

The horizontal and vertical shift coefficients computed by the algorithm are plotted versus temperature in Figs. 9 and 10. The horizontal shift coefficients are fitted by the WLF equation: the parameters $C_1 = 6.71$ and $C_2 = 135.0$ are found to lead to a very good fit. As shown in Fig. 9, the optimised horizontal shift coefficients are really close

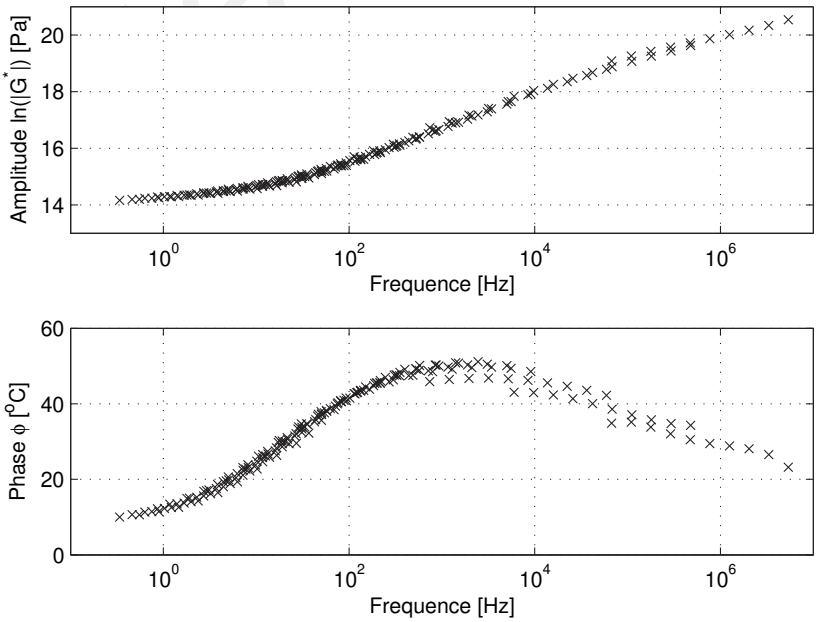

Fig. 6. Master curves for Deltane 350 with a reference temperature of 12 °C.

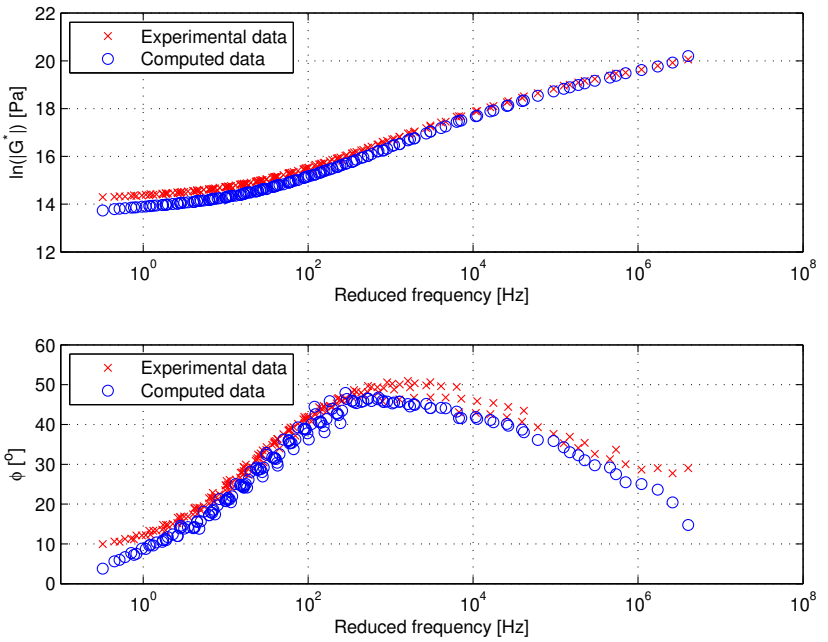

Fig. 7. Comparison between experimental data (crosses) and computed data from the Kramers–Kronig relations (circles) for Deltane 350, at the first optimisation step.

to the starting ones. So the errors observed in Fig. 7 are mostly due to the starting vertical shift coefficients. Indeed, Fig. 10 shows that the temperature dependence of the vertical shift coefficients is not negligible and needs to be taken into account when applying the time–temperature superposition principle. The values of these coefficients are about one order of magnitude smaller than the horizontal shift coefficients, which is coherent with results from the literature (Guedes, 2011; Hatzikiriakos, 2000) and follow a decreasing trend with some scattering. Similar results are obtained by initializing the vertical shift coefficient to those calculated from the Bueche–Rouse equation.

In order to compare the optimised vertical shift coefficients with those predicted by the Bueche–Rouse theory, measurements of the linear thermal expansion coefficient at various temperatures are performed on a TMA 402 F3

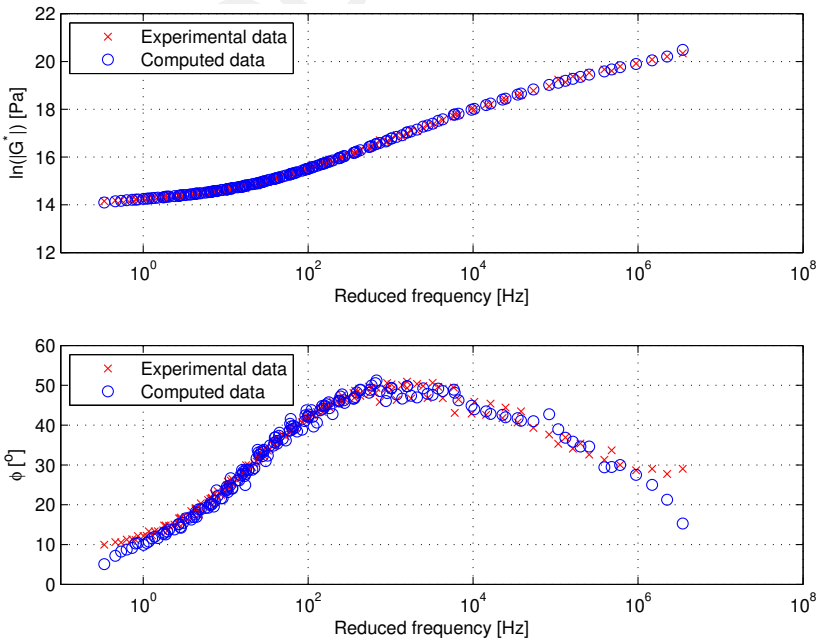

Fig. 8. Comparison between experimental data (crosses) and computed data from the Kramers–Kronig relations (circles) for Deltane 350, at the end of the optimisation.

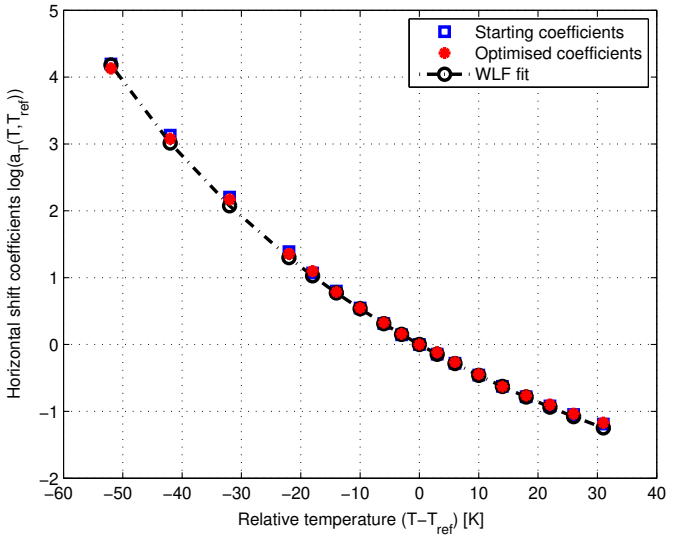

Fig. 9. Horizontal shift coefficients at the first step (squares) and the last step (filled circles) of the optimisation. The optimised coefficients are fitted by the WLF equation (circles).

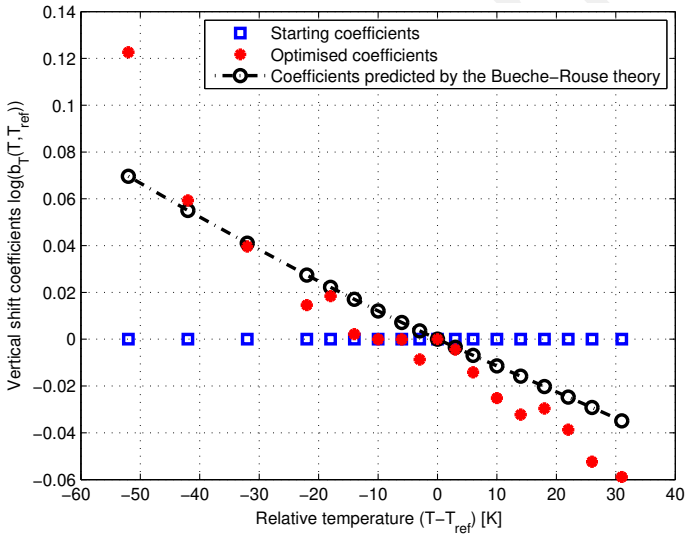

Fig. 10. Vertical shift coefficients at the first step (squares) and the last step (filled circles) of the optimisation are compared with those predicted by the Bueche–Rouse theory (circles).

Hyperion. The vertical shift coefficients calculated from Eq. (14), and using the values of the thermal expansion coefficients measured are plotted on Fig. 10. Except at $T - T_{\text{ref}} = -52$ K where the optimized vertical shift coefficient seems to clearly deviate from the theory, the coefficients computed by the proposed methodology are close enough to those predicted by the Bueche–Rouse theory, and the trend is respected. Experimental errors may be responsible for the single deviation at $T - T_{\text{ref}} = -52$ K and the scattering observed at other temperatures. The limitations of the Bueche–Rouse when applied to filled polymers such as Deltane 350 which contains about 28% of mineral fillers and the possibility of slight non-linearities due to long chain branching which affects the temperature sensitivity of the rheology (Van Gurp and Palmen, 1998; Hatzikiriakos, 2000; Greassley, 1982) are other potential reasons for the scattering and the deviation at $T - T_{\text{ref}} = -52$ K observed.

5. Conclusion

In this work, a method is proposed to calculate the horizontal and vertical shift coefficients allowing the construction of the master curves of a viscoelastic material by application of the time–temperature superposition principle. The originality of this work lies in the least square method used to calculate the horizontal and vertical shift coefficients, which involves the fulfilment of the

Kramers–Kronig relations conveying the causality condition. The method is applied to Deltane 350, a viscoelastic material mostly used in aeronautic applications. The resulting horizontal and vertical shift coefficient are found consistent with the WLF equation, and with previous works. Measurements of the linear thermal expansion coefficients allow to estimate the values of the vertical shift coefficients from the Bueche–Rouse theory. Comparison with the vertical shift coefficients computed by the presented procedure show in general good agreement.

The proposed method presents some advantages over existing methods. Firstly, it provides physical significance to both shift factors, which is not the case in empirical techniques such as hand-shifting and curve fitting techniques. Secondly, it requires less assumptions than other methods also providing physical meaning to the shift coefficients, making it of more general use. For example, some authors are applying methods based on the approximated Kramers–Kronig relations described in Booij and Thoone (1982), which were proved in Parot and Duperray (2007) to introduce significant noise in the results. Another example is the case of methods based on a viscoelastic model (Fowler and Rogers, 2004; Madigosky et al., 2006; Guedes, 2011). This requires to set a priori the material modulus function which might be inappropriate to represent the frequency dependence of the mechanical properties of some materials. Viscoelastic models are generally built to ensure internal consistence, such as causality, so that the master curves obtained by these methods are supposed to verify the Kramers–Kronig relations. These methods can then be seen as a restriction of the shifting procedure presented in this article, since assumptions are made on the material modulus function describing the viscoelastic behaviour.

The temperature shifts applied could be further validated by comparing the master obtained by the presented method to those obtained through other means. Techniques such as broadband viscoelastic spectroscopy or resonant ultrasound spectroscopy allows measurements of the viscoelastic properties over several decades of frequency (Lakes, 2004). New viscoanalysers, making use of piezoelectric actuators, are being developed in order to extend the frequency range of investigation (Renaud et al., 2011) up to 3.5 kHz. This comparison is to be performed in future studies.

Acknowledgments

The financial support of DGA/MRIS (Mission for Scientific Research and Innovation) and DCNS is gratefully acknowledged.

References

01dB-Metravib. Dynatest User Manual DYNATEST.06/NUT/002/B.

Booij, H.C., Thoone, G.P.J.M., 1982. Generalization of Kramers–Kronig transforms and some approximations of relations between viscoelastic quantities. Rheologica Acta 21, 15–24.

Bossemeyer, H.G., 2001. Evaluation technique for dynamic moduli. Mechanics of Time-Dependent Materials 5, 273–291.

Bueche, F., 1954. The viscoelastic properties of plastics. Journal of Chemical Physics 22, 603–609.

Caracciolo, R., Gasparetto, A., Giovagnoni, M., 2001. Applications of causality check and of the reduced variables method for experimental determination of Young's modulus of a viscoelastic material. Mechanics of Materials 33, 693–703.

Chailleux, E., Ramond, G., Such, C., de la Roche, C., 2006. A mathematical-based master-curve construction method applied to complex modulus of bituminous materials. Road Materials and Pavement Design 7, 75–92.

Champeney, D.C., 1973. Fourier Transforms and their Physical Applications. Academic Press.

Christensen, R.M., 2003. Theory of Viscoelasticity. Dover Publication Inc..

Dealy, J., Plazek, D., 2009. Time–temperature superposition – a users guide. Rheology Bulletin 78, 16–31.

Dealy, J., Wissbrun, K.D., 1990. Melt rheology and its role in plastics processing: theory and applications. Van Nostrand Reinhold, New-York.

Emri, I., 2005. Rheology of Solid Polymers. Technical report. The British Society of Rheology.

Enelund, M., Olsson, P., 1999. Damping described by fading memory-analysis and application to fractional derivative models. International Journal of Solids and Structures 36, 939–970.

Ferry, J.D., 1980. Viscoelastic Properties of Polymers. John Wiley & Sons, New-York.

Fowler, B., Rogers, L., 2004. A new approach to temperature shift functions in modeling complex modulus damping data. In: Proceedings of the 75th Shock and Vibration, Symposium.

Fowler, B., Rogers, L., 2006. A new approach to the vertical shift of complex modulus data for damping polymers. In: Proceedings of the 77th Shock and Vibration, Symposium.

Gergesova, M., Zupancic, B., Saprunov, I., Emri, I, 2011. The closed form t-T-P shifting (CFS) algorithm. Journal of Rheology 55, 1–16.

Greassley, W.W., 1982. Effect of long branches on the temperature dependence of viscoelastic properties in polymer melts. Macromolecules 15, 1164–1167.

Guedes, R.M., 2011. A viscoelastic model for a biomedical ultra-high molecular weight polyethylene using the time-temperature superposition principle. Polymer testing 30, 294–302.

Han, C.D., Kim, J.K., 1993. On the use of time-temperature superposition in multicomponent/multiphase polymer systems. Polymer 34, 2533–2539.

Hatzikiriakos, S.G., 2000. Long chain branching and polydiversity effects on the rheological properties of polyethylenes. Polymer Engineering and Science 40, 2279–2287.

Kramers, H.A., 1927. La diffusion de la lumière par les atomes. In Atti del Congresso Internazionale dei Fisici.

Kronig, R. de L., 1926. On the theory of dispersion of X-rays. Journal of the Optical Society of America 12, 547–557.

Lakes, R.S., 2004. Viscoelastic measurement techniques. Review of scientific instruments 75, 797–810.

Madigosky, W.M., Lee, G.F., Niemiec, J.M., 2006. A method for modeling polymer viscoelastic data and the temperature shift function. Journal of the Acoustical Society of America 119, 3760–3765.

Parot, J.-M., Duperray, B., 2007. Applications of exact causality relationships to materials dynamic analysis. Mechanics of Materials 39, 419–433.

Pritz, T., 1999. Verification of local Kramers–Kronig relations for complex modulus by means of fractional derivative model. Journal of Sound and Vibration 228, 1145–1165.

Renaud, F., Chevallier, G., Dion, J.-L., Lemaire, R., 2011. Viscoelasticity measurements and identification of viscoelastic parametric models. In: ASME IDETC, Washington, DC.

Resh, J.A., Stadler, F.J., Kaschta, J., Mnstedt, H., 2009. Temperature dependence of the linear steady-state shear compliance of linear and long-chain branched polyethylenes. Macromolecules 42, 5676–5683.

Sihn, S., Tsai, S.W., 1999. Automated shift for time-temperature superposition. In: Proceedings of the 12th International Committee on Composite Materials.

Silva, H., Gross, B., 1941. Some measurements on the validity of the principle of superposition in solid dielectrics. Physical Review 60, 684–687.

Van Gurp, M., Palmen, J., 1998. Time-temperature superposition for polymeric blends. Rheology Bulletin 67 (1), 5–8.

Williams, M.L., Landel, R.F., Ferry, J.D., 1955. The temperature dependence of relaxation mechanisms in amorphous polymers and other glass-forming liquids. Journal of the American Chemical Society 77, 3701–3707.